

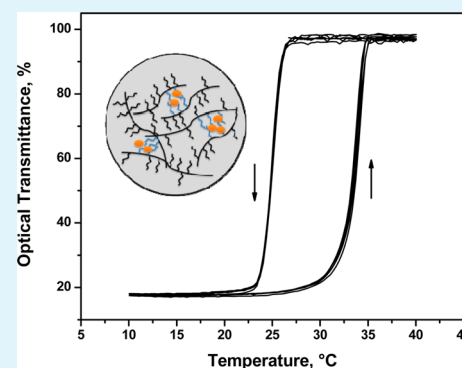
Poly(dodecyl methacrylate) as Solvent of Paraffins for Phase Change Materials and Thermally Reversible Light Scattering Films

Julieta Puig, Roberto J. J. Williams, and Cristina E. Hoppe*

Institute of Materials Science and Technology (INTEMA), University of Mar del Plata and National Research Council (CONICET), Av. J. B. Justo 4302, 7600 Mar del Plata, Argentina

ABSTRACT: Paraffins are typical organic phase change materials (PCM) used for latent heat storage. For practical applications they must be encapsulated to prevent leakage or agglomeration during fusion. In this study it is shown that eicosane ($C_{20}H_{42} = C_{20}$) in the melted state could be dissolved in the hydrophobic domains of poly(dodecyl methacrylate) (PDMA) up to concentrations of 30 wt %, avoiding the need of encapsulation. For a 30 wt % solution, the heat of phase change was close to 69 J/g, a reasonable value for its use as a PCM. The fully converted solution remained transparent at 80 °C with no evidence of phase separation but became opaque by cooling as a consequence of paraffin crystallization. Heating above the melting temperature regenerated a transparent material. A high contrast ratio and abrupt transition between opaque and transparent states was observed for the 30 wt % blends, with a transparent state at 35 °C and an opaque state at 23 °C. This behavior was completely reproducible during consecutive heating/cooling cycles, indicating the possible use of this material as a thermally reversible light scattering (TRLS) film.

KEYWORDS: eicosane, paraffin, phase change material (PCM), poly(dodecyl methacrylate), thermally reversible light scattering film (TRLS)



1. INTRODUCTION

One of the proposed technologies for the storage of thermal energy involves the use of phase change materials (PCMs).^{1–13} These materials make use of latent energy; e.g., crystalline materials absorb energy during melting and release energy during crystallization. Paraffins are typical organic PCMs due to several advantages: low cost, low toxicity, high heat of fusion, chemical inertness, low vapor pressure, small volume change on melting, congruent melting, and self-nucleating properties.^{1–13} However, for practical applications they must be encapsulated to prevent leakage and agglomeration during fusion.^{14–23} Otherwise, special containers must be designed for this purpose.^{24,25}

In this study, the possibility of using poly(*n*-alkyl methacrylates) with long side chains to dissolve melted paraffins is analyzed. As the polar polymer backbone does not have chemical affinity with the hydrophobic side chains, a nanostructuring of the amphiphilic polymer takes place, generating nanodomains of associated side chains.^{26,27} At sufficiently low temperatures, partial crystallization of side chains occurs in these nanodomains.²⁷ The question we ask is if melted paraffins can be reversibly dissolved in nanodomains of *n*-alkyl chains. Paraffins should be expelled during crystallization and redissolved after melting in the course of cooling/heating cycles of the material. Above the melting temperature of the paraffin the material should be transparent, and below the crystallization temperature the material should become opalescent/opaque due to the scattering of light by paraffin

crystals. Therefore, the material may be useful both as a PCM and as a thermally reversible light scattering (TRLS) film. Optical properties of TRLS films based on encapsulated organic crystals dispersed in a polymer matrix have been reported.^{28,29}

The selected paraffin was eicosane, $C_{20}H_{42}$ (C_{20}), and the amphiphilic polymer was poly(dodecyl methacrylate) (PDMA), also identified as poly(lauryl methacrylate). Materials containing up to 30 wt % C_{20} in PDMA were obtained by free radical polymerization of solutions of C_{20} in dodecyl methacrylate. Thermal and optical properties of the resulting materials were analyzed to determine their potential use as PCM or TRLS films. A rheological characterization evidenced the dissolution of melted C_{20} in hydrophobic domains of PDMA.

2. MATERIALS AND METHODS

The monomer dodecyl methacrylate (DMA, Fluka, 95%) was used as received. It contained 500 ppm of *p*-methoxyphenol as inhibitor. The initiator was benzoyl peroxide (BPO, Akzo-Nobel). The selected paraffin was normal eicosane, $C_{20}H_{42}$ (C_{20} , Aldrich, 99%), with a melting temperature range of 35–37 °C. Tetrahydrofuran (THF, Biopack) was P.A. grade.

Polymerization of DMA/ C_{20} Solutions. A solution of DMA containing 2 wt % BPO (with respect to DMA) and C_{20} (0–30 wt % with respect to the total mass) was sonicated at 40 °C until the paraffin was melted and completely dissolved. The free-radical polymerization

Received: July 5, 2013

Accepted: August 26, 2013

Published: August 26, 2013

was performed at 80 °C under nitrogen flow in a sealed silicon mold, between glass covers, or in the cell of a characterization device. The thickness of the films obtained between two glass covers was selected based on potential application of these materials as a constitutive part of a glass smart window with a sharp transparent–opaque transition and PCM properties. To adjust the thickness (200, 500, and 1000 μm), steel spacers were placed between the two glass covers and liquid precursors casted to completely fill the space between them. Under this procedure, complete coverage of the surface and uniformity in thickness was easily achieved. The size of these glass covers was selected to fill the requirements of subsequent characterization procedures. For microscopy measurements, 1.2 cm diameter rounded glass covers were used to allow thermal cycling in a hot stage. Bulky samples were obtained by curing liquid precursors in a sealed silicon mold under nitrogen flow. These samples could be peeled off using tweezers to obtain free-standing materials.

Characterization Techniques. The polymerization kinetics was determined by Fourier-transformed near-infrared spectroscopy using an FT-NIR device (Nicolet 6700), provided with a heated transmission cell (HT-32, Spectra Tech) and a temperature controller (CAL 9500P, Spectra Tech). The sample was placed between glass windows using a rubber spacer of 1.4 mm thickness. The height of the absorption band at 6165 cm^{-1} was used to determine the conversion of methacrylate double bonds as a function of time at 80 °C, for solutions of different C20 contents.

Differential scanning calorimetry (DSC, Pyris 1, Perkin-Elmer and TA Q2000 Thermal Analysis) was used to determine heats and temperatures of fusion and crystallization for samples previously polymerized to full conversion. Dynamic scans were performed at 10 °C/min, circulating nitrogen outside the sealed pans.

Optical properties of samples polymerized between two glass covers were determined by transmission optical microscopy (TOM) at different heating/cooling rates. A Leica DMLB microscope was employed provided with a hot stage (Linkman THMS 600) and a photodetector in the optical path.

The evolution of the storage (G') and loss modulus (G'') of fully converted samples was followed using an Anton Paar rheometer (model Physica MCR-301) provided with a CTD 600 thermo-chamber. Solutions were polymerized at 80 °C, in the same device, for the period of time necessary to attain full conversion (corroborated by FT-NIR spectra). Dynamic scans were performed at 2 °C/min, cooling from 80 to -40 °C and heating again to 80 °C. A parallel-plate configuration (diameter = 25 mm, gap \approx 1 mm) was used in oscillatory mode with a 1% amplitude, at a frequency of 1 Hz.

Scanning electron microscopy (SEM, JEOL JSM-6460LV) was used to observe the morphology of cryogenically fractured samples. Samples were previously coated with Au–Pd.

3. RESULTS AND DISCUSSION

3.1. Polymerization Kinetics. The conversion of methacrylate groups at 80 °C was followed by the decrease in the intensity of its absorption band at 6165 cm^{-1} in FT-NIR spectra.³⁰ Figure 1 shows conversion vs time curves for the neat DMA monomer and for a solution containing 30 wt % C20. In spite of the high C20 concentration, the evolution of conversion was very close for both samples up to conversions in the range of 40%. From this point on, the solution containing C20 exhibited a slower polymerization rate.

The question arises about the absence of a dilution effect on the initial polymerization rate produced by the presence of 30 wt % C20. A trivial explanation would be that the paraffin was not dissolved by DMA at 80 °C. As both components have different refractive indices, an opalescent/opaque solution would have resulted. However, this was not the case. Besides, it has been reported that DMA is a good solvent of polyethylene above its melting temperature.³¹ Therefore, it must also be a good solvent of C20 above its melting point. An

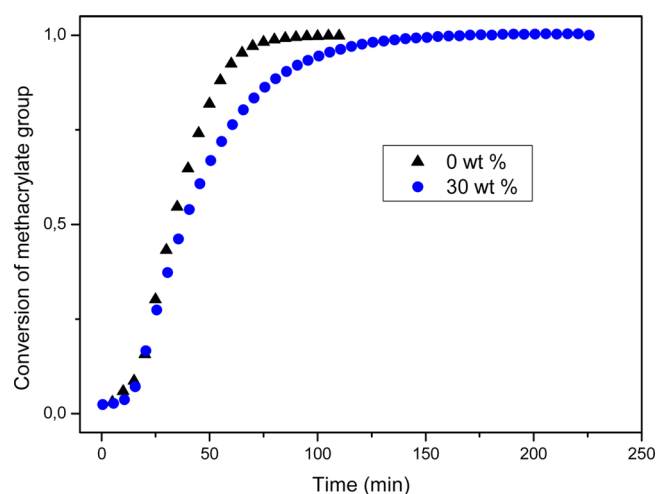


Figure 1. Evolution of the conversion of methacrylate double bonds at 80 °C for the neat monomer and for a solution containing 30 wt % C20.

alternative explanation arises from the description of the free-radical polymerization of nanostructured monomers. It has been proposed that the polymerization occurs first in disordered domains and then in the organized domains produced by the association of dodecyl chains.^{32,33} Assuming that C20 is dissolved in the hydrophobic nanodomains generated by the association of dodecyl chains of DMA, the initial polymerization stage taking place in disordered domains would not be affected, in agreement with the experimental observation.

3.2. Physical Properties of the C20/PDMA Solutions Polymerized to Full Conversion. Samples containing up to 30 wt % C20 and polymerized to full conversion (within the experimental error of FT-NIR) remained transparent at 80 °C with no evidence of phase separation. It can be inferred that paraffin remained dissolved in the hydrophobic domains formed by dodecyl chains. Crystallization of C20 was produced when cooling the fully polymerized samples to room temperature, as revealed by TOM observations. This turned samples from a transparent to an opalescent/opaque state. Heating above the melting temperature of C20 crystals led again to a transparent solution in a completely reversible way.

Some authors reported that secondary reactions involving generation and recombination of radicals in pendant dodecyl chains could lead to a chemically cross-linked PDMA.^{34,35} However, under our polymerization conditions, neat PDMA samples and blends with C20 were completely soluble in THF at room temperature.

3.3. C20/PDMA Blends as Phase Change Materials (PCM). Crystallization and melting of C20 in blends with PDMA were investigated by DSC. As an example, Figure 2 shows thermograms obtained in cooling and heating cycles for a blend containing 30 wt % PDMA. The extremes of both peaks were located at 34 °C (melting) and 29 °C (crystallization). The behavior was reversible in consecutive heating/cooling cycles.

Crystallization and melting temperatures, taken at the maximum (minimum) of the broad peaks, increased with the C20 contents up to 30 wt %, as shown in Figure 3. This is a proof of the solubility of C20 in PDMA in this concentration range. The values of neat C20 are also indicated, but these points are not joined with those in the low concentration range

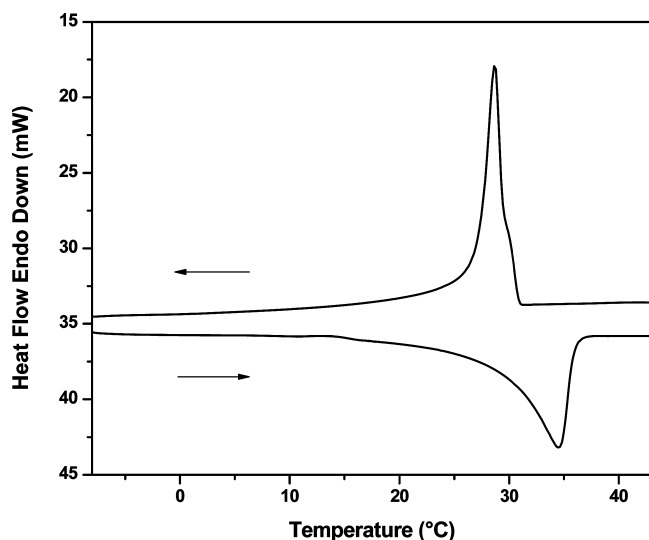


Figure 2. DSC thermograms obtained in cooling and heating steps for a C20/PDMA blend containing 30 wt % C20.

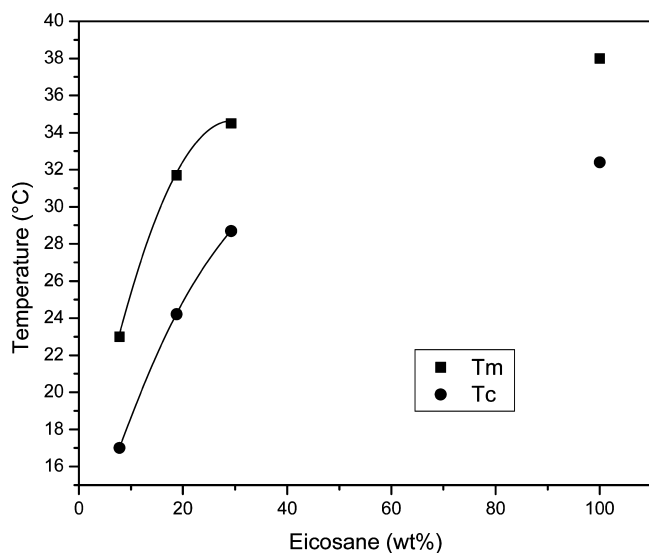


Figure 3. Crystallization (T_c) and melting (T_m) temperatures of pure C20 and C20/PDMA blends of different concentrations up to 30 wt % C20, determined as the maximum (minimum) of the peaks in DSC thermograms.

because a liquid–liquid phase separation could take place at high C20 concentrations.^{31,36}

Within the experimental error of DSC determinations, for a particular C20 concentration the heat of melting was equal to the heat of crystallization. The blend containing 30 wt % C20 showed a heat of phase change equal to 69 J/g, a reasonable value for a phase change material based on microencapsulated paraffins.^{21–23,37,38} The experimental value determined for neat C20 was 254 J/g. Therefore, the theoretical value for the 30 wt % blend was 76 J/g. This means that about 90% of C20 present in the blend could be crystallized. Crystallinity values above 90% can be commonly found in the literature for PCM materials. For example, in the case of blends containing 40 wt % of a technical paraffin in a styrene–butadiene–styrene (SBS) copolymer, a crystalline fraction of paraffin close to 97% was reported, with lower values expected by decreasing the paraffin amount.⁴

3.4. C20/PDMA Blends as Thermally Reversible Light Scattering Films (TRLS). Regarding the use of these materials as TRLS films, it is necessary to evaluate the optical contrast between transparent and opaque states, the corresponding switching temperatures, and the reproducibility during consecutive cooling/heating cycles. As an example, Figure 4a shows the optical transmittance of a 200 μm thickness film of a blend containing 30 wt % C20, submitted to a heating and cooling cycle at 20 $^\circ\text{C}/\text{min}$.

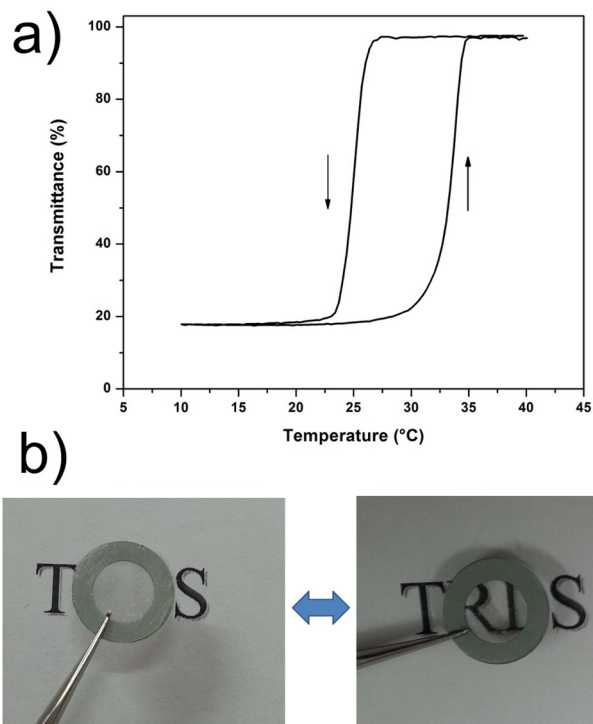


Figure 4. (a) Optical transmittance as a function of temperature for a 200 μm thick film containing 30 wt % C20, submitted to a heating/cooling cycle at 20 $^\circ\text{C}/\text{min}$. (b) Optical images of the TRLS films in the opaque (left) and transparent (right) states.

The film became opaque in the 27–23 $^\circ\text{C}$ range during the cooling stage and transparent in the 30–35 $^\circ\text{C}$ range during the heating step (Figure 4b). Figure 5 shows SEM and TOM micrographs of the samples in the opaque state and an optical image of the sample obtained as a free-standing thick sample.

Microscopic analysis (Figures 5a and 5b) showed that at room temperature samples were constituted by a fine dispersion of micrometric crystals uniformly distributed in the polymer matrix. This characteristic size and uniform distribution of crystals were responsible for the efficient scattering of visible light and for the opaque appearance of the samples at room temperature (Figure 5c). The opaque–transparent switching behavior occurred with a high reproducibility for successive heating–cooling cycles, as shown in Figure 6. This evidences the absence of leakage or agglomeration of the paraffin during the consecutive thermal cycles.

The contrast ratio was very much affected by the heating/cooling rate. Figure 7 shows the effect of changing the rate from 20 to 1 $^\circ\text{C}/\text{min}$. At low temperatures the material obtained by cooling at 1 $^\circ\text{C}/\text{min}$ was opalescent rather than opaque, producing a significant decrease of the contrast ratio. TOM observations showed a decrease of the average crystal size when

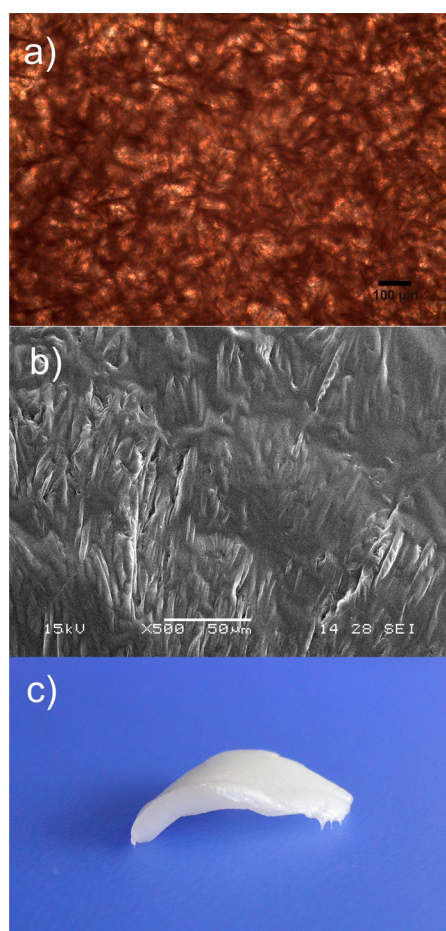


Figure 5. (a) TOM and (b) SEM micrographs of a 200 μm thickness film and a 1 mm thick sample, respectively, containing 30 wt % C20, submitted to a heating/cooling cycle at 20 $^{\circ}\text{C}/\text{min}$. (c) Optical image of a piece of free-standing thick sample containing 30 wt % C20.

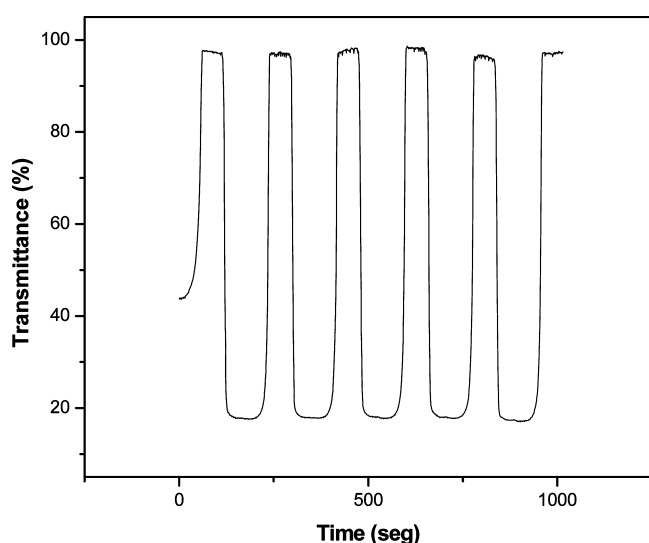


Figure 6. Intensity of transmitted light as a function of time during successive heating/cooling cycles at 20 $^{\circ}\text{C}/\text{min}$, for a 200 μm thick film containing 30 wt % C20.

increasing the cooling rate, a fact explained by the competition between nucleation and growth rates.³⁹ As smaller crystals are more effective for scattering visible light, the result is an

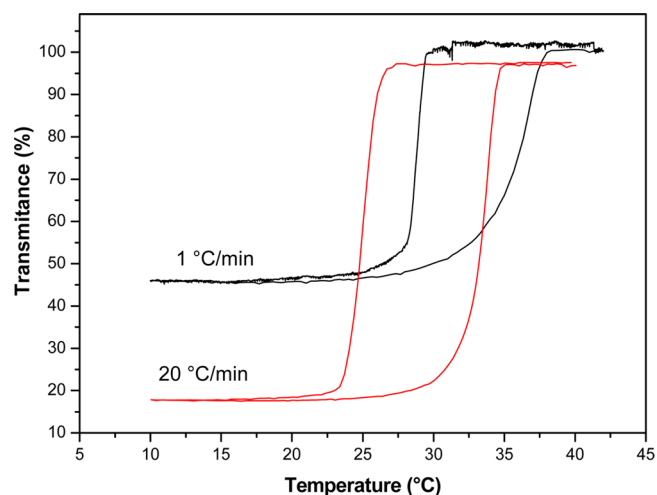


Figure 7. Optical transmittance as a function of temperature for a 200 μm thick film containing 30 wt % C20, submitted to heating/cooling cycles of 1 and 20 $^{\circ}\text{C}/\text{min}$.

increase in the opacity with the increase in the cooling rate. Obviously, increasing the film thickness produced an enhancement of the contrast ratio at low cooling rates.

3.5. Rheological Evidence of the Dissolution of C20 in Hydrophobic Domains. Extra evidence of the fact that C20 in the melted state remains dissolved in hydrophobic domains was provided by rheological tests. Figure 8 shows the evolution

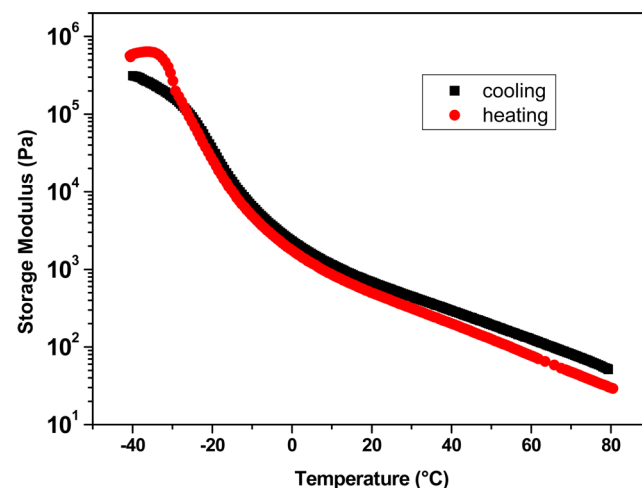


Figure 8. Variation of the storage modulus of neat PDMA during a cooling/heating cycle at 2 $^{\circ}\text{C}/\text{min}$.

of the storage modulus of neat PDMA when cooled from 80 to -40 $^{\circ}\text{C}$, followed by a consecutive heating to 80 $^{\circ}\text{C}$. The behavior is essentially reversible. A 4-decades increase of the storage modulus, from the range of 10 – 10^2 Pa to the range of 10^5 – 10^6 Pa, is observed during the cooling stage. At 80 $^{\circ}\text{C}$ the solution was a liquid ($G'' > G'$), and it became a physical gel at low temperatures ($G' > G''$). The reversible formation of a physical gel is ascribed to the self-association of the pendant dodecyl chains of the linear PDMA.^{26,27,40}

Solutions of C20 in PDMA exhibited a completely different rheological behavior as shown in Figure 9 for a blend containing 20 wt % C20. The storage modulus in the liquid state was much lower than the one of neat PDMA. In the 30–80 $^{\circ}\text{C}$ range, it was comprised between 1 and 10 Pa. This is

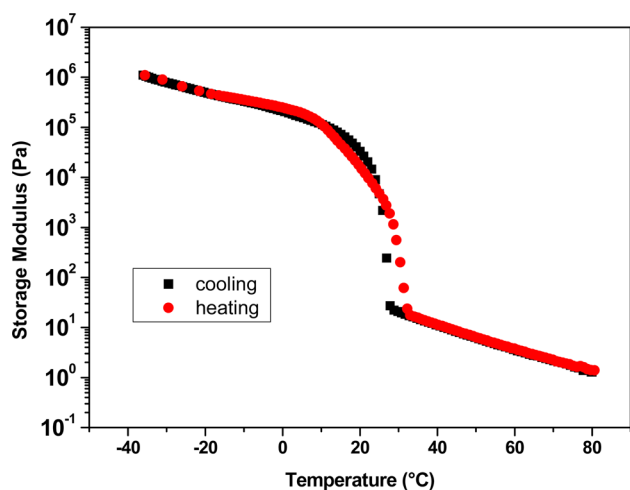


Figure 9. Variation of the storage modulus of a C20/PDMA blend containing 20 wt % C20, during a cooling/heating cycle at 2 °C/min.

assigned to the dissolution of C20 in hydrophobic domains, a fact that decreased the fraction of self-associated pendant chain and, consequently, the average molar mass of polymer chain aggregates. A diminution of the molar mass of polymer aggregates produces a corresponding decrease of the storage modulus.⁴¹

A very sharp increase of the modulus is observed at the crystallization temperature of C20, attaining values comprised in the range of 10^5 – 10^6 Pa with further cooling. The phase separation of C20 enabled the rapid self-association of pendant dodecyl chains with a corresponding increase of the storage modulus. At low temperatures the material was a physical gel ($G' > G''$), reinforced by C20 crystals and with the mechanical properties of a soft elastomer ($G' \sim 0.1$ MPa).

The self-associated pendant dodecyl chains of PDMA can form small crystalline domains under cooling.²⁷ Reported values for the melting temperature and the heat of fusion were -26 °C and 2 kJ/mol of dodecyl chains.²⁷ This corresponded to a 6% fraction of CH_2 groups in crystalline domains. To corroborate the presence of this small peak in our materials, DSC scans of samples previously cooled to -60 °C were performed (Figure 10). A small endothermic peak with a minimum at about -33 °C was observed for both the neat PDMA and a blend containing 30 wt % C20. The heat of fusion was 2.1 kJ/mol of dodecyl chains for both samples, in agreement with the value reported in the literature.²⁷ This result corroborates the fact that in blends containing C20 pendant dodecyl chains self-associate after crystallization of the paraffin. Above melting temperature of the paraffin (about 35–40 °C) the system behaves as a viscoelastic liquid with a very high concentration of alkyl chains and high viscosity that acted very efficiently as an encapsulation medium of the liquid paraffin. This was demonstrated by the absence of leakage and macrophase separation even after several cooling–heating cycles.

CONCLUSIONS

Eicosane (C20) in the melted state could be dissolved in hydrophobic domains of poly(dodecyl methacrylate) (PDMA), in concentrations up to 30 wt %. When the solution was cooled, crystallization of C20 produced its segregation from hydrophobic domains and the self-association of pendant dodecyl chains of the linear polymer. A physical gel reinforced with C20

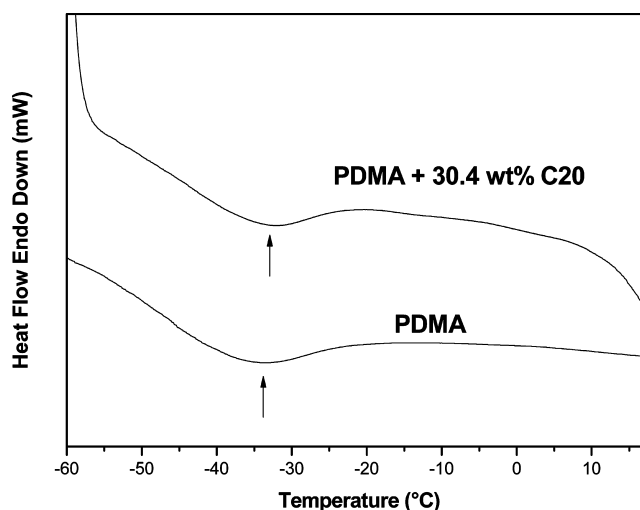


Figure 10. DSC heating scans of neat PDMA and of a blend with 30 wt % C20 previously cooled to -60 °C.

crystals was generated, with a storage modulus comprised between 0.1 and 1 MPa. Heating this material above the melting temperature of C20 regenerated a liquid solution. This behavior was completely reversible in consecutive cooling/heating cycles, suggesting the possible use of these solutions as phase change materials (PCM) or thermally reversible light scattering films (TRLS). A 30 wt % C20 content was suitable for these purposes.

Results obtained in this study for a model system (C20/PDMA) could be extended to blends of cheaper paraffins (e.g., paraffin waxes) with different types of poly(*n*-alkyl methacrylates). Blends can be prepared by in situ polymerization of the monomer in the presence of the paraffin, as in the present study, or by direct mixing the paraffin and the polymer. Optical and thermal properties of the resulting materials might be varied in a wide range.

AUTHOR INFORMATION

Corresponding Author

*E-mail: hoppe@fi.mdp.edu.ar. Phone: +54-223-481-6600.

Notes

The authors declare no competing financial interest.

ACKNOWLEDGMENTS

The financial support of the National Research Council (CONICET), the University of Mar del Plata, and the National Agency for the Promotion of Science and Technology (ANPCyT) is gratefully acknowledged.

REFERENCES

- (1) Sharma, A.; Tyagi, V. V.; Chen, C. R.; Buddhi, D. *Renewable Sustainable Energy Rev.* **2009**, *13*, 318–345.
- (2) Kenisarin, M. M.; Kenisarina, K. M. *Renewable Sustainable Energy Rev.* **2012**, *16*, 1999–2040.
- (3) Rathod, M. K.; Banerjee, J. *Renewable Sustainable Energy Rev.* **2013**, *18*, 246–258.
- (4) Xiao, M.; Feng, B.; Gong, K. *Energy Convers. Manage.* **2002**, *43*, 103–108.
- (5) Inaba, H.; Tu, P. *Heat Mass Transfer* **1997**, *32*, 307–312.
- (6) Mehrali, M.; Latibari, S. T.; Mehrali, M.; Metselaar, H. S. C.; Silakhori, M. *Energy Convers. Manage.* **2013**, *67*, 275–282.
- (7) Sun, Z.; Kong, W.; Zheng, S.; Frost, R. L. *Sol. Energy Mater. Sol. Cells* **2013**, *117*, 400–407.

- (8) Zhang, Z.; Shi, G.; Wang, S.; Fang, X.; Liu, X. *Renewable Energy* **2013**, *50*, 670–675.
- (9) Zhang, P.; Hu, Y.; Song, L.; Ni, J.; Xing, W.; Wang, J. *Sol. Energy Mater. Sol. Cells* **2010**, *94*, 360–365.
- (10) Li, H.; Fang, G.; Liu, X. *J. Mater. Sci.* **2010**, *45*, 1672–1676.
- (11) Ehid, R.; Fleischer, A. S. *Energy Convers. Manage.* **2012**, *53*, 84–91.
- (12) Cheng, W. L.; Zhang, R. M.; Xie, K.; Liu, N.; Wang, J. *Sol. Energy Mater. Sol. Cells* **2010**, *94*, 1636–1642.
- (13) Sun, Z.; Zhang, Y.; Zheng, S.; Park, Y.; Frost, R. L. *Thermochim. Acta* **2013**, *558*, 16–21.
- (14) Hawlader, M. N. A.; Uddin, M. S.; Zhu, H. J. *Int. J. Solar Energy* **2000**, *20*, 227–238.
- (15) Zhang, X. X.; Tao, X. M.; Yick, K. L.; Fan, Y. F. *J. Appl. Polym. Sci.* **2005**, *97*, 390–396.
- (16) Su, J. F.; Huang, Z.; Ren, L. *Colloid Polym. Sci.* **2007**, *285*, 1581–1591.
- (17) Jin, Z. G.; Wang, Y. D.; Liu, J. G.; Yang, Z. Z. *Polymer* **2008**, *49*, 2903–2910.
- (18) Hong, Y.; Ding, S.; Wu, W.; Hu, J.; Voevodin, A. A.; Gschwender, L.; Snyder, E.; Chow, L.; Su, M. *ACS Appl. Mater. Interfaces* **2010**, *2*, 1685–1691.
- (19) Phadungphatthanakoon, S.; Poompradub, S.; Wanichwecharungruang, S. P. *ACS Appl. Mater. Interfaces* **2011**, *3*, 3691–3696.
- (20) Basal, G.; Deveci, S. S.; Yalcin, D.; Bayraktar, O. *J. Appl. Polym. Sci.* **2011**, *121*, 1885–1889.
- (21) Alkan, C.; Sari, A.; Karaipekli, A. *Energy Convers. Manage.* **2011**, *52*, 687–692.
- (22) Qiu, X.; Li, W.; Song, G.; Chu, X.; Tang, G. *Energy* **2012**, *46*, 188–199.
- (23) Mochane, M. J.; Luyt, A. S. *Thermochim. Acta* **2012**, *544*, 63–70.
- (24) Parameshwarana, R.; Kalaiselvamb, S.; Harikrishnanb, S.; Elayaperumala, A. *Renewable Sustainable Energy Rev.* **2012**, *16*, 2394–2433.
- (25) Ostermana, E.; Tyagib, V. V.; Butalaa, V.; Rahimb, N. A.; Stritih, U. *Energy Build* **2012**, *49*, 37–49.
- (26) Beiner, M.; Schröter, K.; Hempel, E.; Reissig, S.; Donth, E. *Macromolecules* **1999**, *32*, 6278–6282.
- (27) Hempel, E.; Huth, H.; Beiner, M. *Thermochim. Acta* **2003**, *403*, 105–114.
- (28) Zucchi, I. A.; Galante, M. J.; Williams, R. J. J. *Eur. Polym. J.* **2006**, *42*, 815–822.
- (29) Zucchi, I. A.; Resnik, T.; Oyanguren, P. A.; Galante, M. J.; Williams, R. J. J. *Polym. Bull.* **2007**, *58*, 145–151.
- (30) Stansbury, J. W.; Dickens, S. H. *Dent. Mater.* **2001**, *17*, 71–79.
- (31) l’Abee, R.; Goossens, H.; van Duin, N.; Spoelstra, A. *Eur. Polym. J.* **2009**, *45*, 503–514.
- (32) Kargin, V. A.; Kabanov, V. A. *Zh. Vses. Khim. O-va. im. D. I. Mendeleeva* **1964**, *9*, 602–631.
- (33) Jašo, V.; Radičević, R.; Stoilković, D. *J. Therm. Anal. Calorim.* **2010**, *101*, 1059–1063.
- (34) Lazár, M.; Hřčková, L.; Fiedlerová, A.; Borsig, E. *Macromol. Mater. Eng.* **2000**, *283*, 88–92.
- (35) Lazár, M.; Hřčková, L.; Borsig, E. *J. Macromol. Sci., Part A: Pure Appl. Chem.* **2002**, *A39*, 365–377.
- (36) Goossens, J. G. P. Processing of tractable polymers using reactive solvents. *PhD Thesis*, Eindhoven University of Technology, The Netherlands, 1998.
- (37) Sari, A.; Alkan, C.; Karaipekli, A. *Appl. Energy* **2010**, *87*, 1529–1534.
- (38) Su, J. F.; Wang, L. X.; Ren, L. *Colloid Surf. A* **2007**, *299*, 268–275.
- (39) Venkatesan, R.; Nagarajan, N. R.; Paso, K.; Yi, Y. B.; Sastry, A. M.; Fogler, H. S. *Chem. Eng. Sci.* **2005**, *60*, 3587–3598.
- (40) Puig, J.; Zucchi, I. A.; Hoppe, C. E.; Pérez, C. J.; Galante, M. J.; Williams, R. J. J.; Rodríguez-Abreu, C. *Macromolecules* **2009**, *42*, 9344–9350.
- (41) Ferry, J. D. *Viscoelastic Properties of Polymers*, 3rd ed.; Wiley: New York, USA, 1980; p 228.